



DFNS/ α -CD/Au as a Nanocatalyst for Interpolation of CO₂ into Aryl Alkynes Followed by S_N² Coupling with Allylic Chlorides

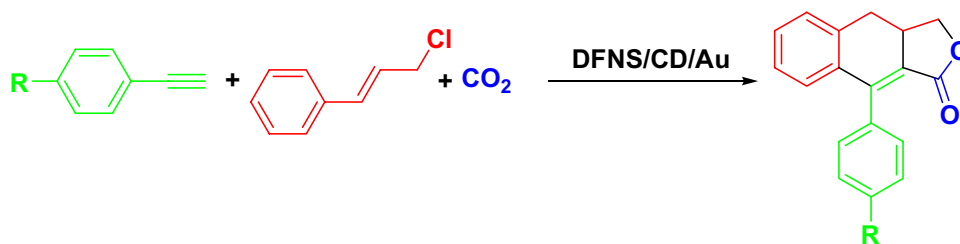
Zhiyong Wang¹ · Xuhao Li² · Li Feng² · Bingzhi Liu² · Farzaneh Shamsa³

Received: 18 August 2020 / Accepted: 1 November 2020
 © Springer Science+Business Media, LLC, part of Springer Nature 2020

Abstract

In the present study, to effectively carbonylate cinnamyl chloride and phenylacetylene with CO₂, α -cyclodextrin doping dendritic fibrous nanosilica (DFNS) supported nanoparticles of gold was used as a catalyst (DFNS/ α -CD/Au NPs). In the catalyst, the nanoparticles of Au were in situ reduced on the surfaces of DFNS. Transmission electron microscopy (TEM), scanning electron microscope (SEM), X-ray diffraction (XRD), Fourier transform infrared spectroscopy (FT-IR), and X-ray energy dispersive spectroscopy (EDS) were utilized for characterizing the nanostructures DFNS/ α -CD/Au. It was found that the nanostructures of DFNS/ α -CD/Au can be nominated due to their effective and novel catalytic behaviour during the synthesis of 3a,4-dihydronaphtho[2,3-c] furan-1(3H)-ones from cinnamyl chloride, phenylacetylene, and CO₂.

Graphic Abstract



Keywords Nanocatalyst · Green chemistry · One-pot synthesis · Nanoparticle · Carbon dioxide

1 Introduction

The conservation of CO₂ to beneficial organic chemicals has been extensively researched by scientists [1–5]. In the chemical industry, the transportation sector, and power plants, CO₂ is known as a greenhouse gas and a waste compound [6, 7]. In addition, it is non-toxic, non-flammable, inexpensive, and easily available carbon feedstock [8, 9]. However, CO₂ is not generally used in the industry due to its low reactivity [10]. Optimal reaction conditions, significant energy input, and highly active catalysts are key factors for the appropriate conversion of stable thermodynamic CO₂ molecules [11]. Rawat et al. reported the synthesis of MgO@Ag-7 as a new catalyst for the placement of CO₂ into aryl alkynes, followed by S_N² binding with allylic chlorides to prepare a wide range of ester and lactone heterocycles in excellent efficiency for

✉ Zhiyong Wang
weeklywang@163.com

✉ Li Feng
fl19860314@126.com

✉ Farzaneh Shamsa
Farzaneh.Shamsa@gmail.com

¹ Department of Basic Course, Shenyang University of Technology, Liaoyang 111003, Liaoning, China

² School of Civil and Transportation Engineering, Guangdong University of Technology, Guangzhou 510006, Guangdong, China

³ Young Researchers and Elite Club, Neyshabur Branch, Islamic Azad university, Neyshabur, Iran

the first time [12]. Many of these naturally occurring furan and annulated furan derivatives and their unnatural analogs have a wide range of biological activity and are important precursors for the synthesis of natural products. [13, 14] Especially, naphtho [2,3-b] furan-4,9-dione derivatives as represented by avicquinones [15] and maturinones [16] have shown a diversity of biological activities of medical importance, such as anticancer, antibacterial and anti-inflammatory activity [17].

The employment of new metal NPs in catalysis has long attracted the attention of researchers due to their robust catalytic activities [18–22]. Among the reported metal nanoparticles deployed in catalysis, Au nanoparticles are the most resistant metal nanoparticles, and have been considerably researched due to their size-related characteristics that can be used in different implementations [23–33]. This characteristic can decrease the yield of the catalysts. To address this weakness, gold nanoparticles are usually fixed on solid supports with mesopores, including Al_2O_3 [34–36], SBA-15 [37–39], SBA-16 [40], and MCM-41 [41, 42]. When employing one of these Au-supported catalysts, small Au NPs are mainly intersperse on internal surfaces and pores. As a result, active sites within the pores are not easily accessible, which limits their applications. Therefore, catalyst support with good availability and high surface areas (i.e. not inside the pores) is extremely advantageous. Access to active gold sites in mesoporous silica was limited because of the normal tubular anatomy and the blockage of the pores, reducing the overall catalyst activity. Therefore, there is an immediate need for a resistant catalyst. Considering our previous study on nanocatalysis, [43, 44] we decided to use dendritic fibrous nanosilica (DFNS).

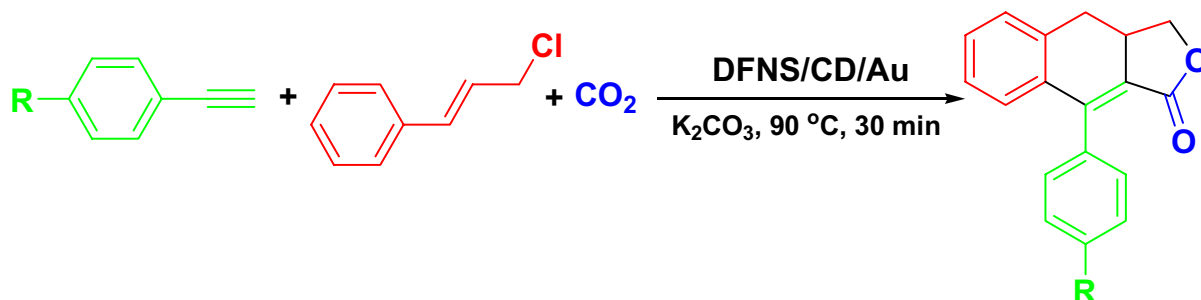
Recently, dendritic fibrous nanosilica has been discovered by Polshettiwar et al. [45–48]. It has illustrated exceptional activities from all angles, such as gas absorption, catalysis, energy storage, solar-energy harvesting, biomedical applications and sensors. It is called fibrous Nanosilica (KCC-1) because of the fibrous structure of it in our main report [49–53]. Nevertheless, the fibres were thin sheets 3.5–5.2 nm thick and therefore, many other names are utilized in the

literature to call them, including wrinkled, fibrous, dendritic, Nanoflower, lamellar, and dandelion. Recently, cyclodextrins (CD) have been used for the preparation of supported metal or metal oxide catalysts [54–58]. These polyhydroxylated compounds are able to stabilize host-guest complexes and molecule-ion adducts with inorganic metal salts [57–61]. In this Review, to avoid confusion, an attempt has been made to consider the same name utilized in the respective original works. However, for ease of reading, we use dendritic fibrous nanosilica (DFNS) for this class of materials [62]. Therefore, α -cyclodextrin (α -CD) supported on the DFNS surface, called DFNS/ α -CD, were produced and utilized to construct DFNS supported gold NPs (DFNS/ α -CD/Au) catalysts by reducing Au on the surface of DFNS. The α -CD compound was employed in the anatomy of a catalyst to avoid nanoparticles from leaching. In the case of the DFNS/ α -CD/Au catalyst, Au NPs supported on DFNS can be used for the synthesis of 3a, 4-dihydronaphtho [2,3-c] furan-1(3H)-ones from cinnamyl chloride, phenylacetylene, and CO_2 demonstrating the positive promoting influence of Au NPs (Scheme 1). This indicates the high catalytic power of gold nanoparticles to perform this reaction.

2 Experimental

3 Materials and Methods

Highly pure chemicals were bought from Fluka and Merck. Melting points in open capillaries were discovered employing an Electrothermal 9100 apparatus and were not corrected. FTIR spectra were identified on a VERTEX 70 spectrometer (Bruker) in the transmission mode in spectroscopic grade KBr pellets for powders. Particle size and nanoparticle anatomy were perceived employing a Philips CM10 transmission electron microscope working at 100 kV. X-ray diffraction data were acquired deploying Bruker D8 Advance model with Cu $\text{K}\alpha$ radiation. Thermogravimetric



Scheme 1 Synthesis of 3a,4-dihydronaphtho[2,3-c]furan-1(3H)-ones in the presence of DFNS/ α -CD/Au NPs

analysis (TGA) was performed on NETZSCH STA449F3 at 10 °C min⁻¹ under nitrogen. The concentrations of Au element and Ag element were measured by Varian 710 inductively coupled plasma spectrometry (ICP-MS). The samples for ICP were dissolved in aqua regia (HCl/HNO₃). Product purification and reaction controlling were performed by TLC on silica gel polygram SILG/UV 254 plates.

3.1 Universal Approach for the Synthesis of the DFNS NPs

First, 3.0 g of tetraethyl orthosilicate (TEOS) was dissolved in cyclohexane (25 mL) and 1-pentanol (1.0 mL) solutions. Then, cetylpyridinium bromide (CPB) (1.2 g) and urea (0.7 g) were stirred in a constant amount of water (25 mL), and added. The blend was stirred continuously at 25 °C for 45 min. After adjusting in a Teflon-sealed autoclave, it was heated at 110 °C for 4 h. The produced silica was separated and centrifuged, washed using an acetone-deionized water mixture, and dried utilizing a drying oven. In the presence of air, the produced material was calcined at 500 °C for 4 h.

3.2 Universal Approach to the Synthesis of the N-Phenylaminomethyl-Modified NPs

24 mg aniline (0.2 mmol) was added in anhydrous *N,N'*-dimethylformamide (DMF, 2.2 mL). Then, 4 mg Tetrabutylammonium iodide as well as 0.3 mL anhydrous NEt₃ were released in the solution. Next, chloromethyltrimethoxysilane (30 μ L) was released. The solution was heated to 70 °C in the presence of N₂ gas for 24 h. The solvent was detached. The resulting mixture was added to a suspension of PhMe/EtOH (1 mL EtOH as was as 40 mL PhMe) and a constant amount of as-synthesized DFNS (200 mg). After that, the suspension was refluxed under the attendance of N₂ gas for 12 h, centrifuged, and washed using MeOH. Finally, the reaction mixture was refluxed for 12 h in the presence of N₂ gas. The material was centrifuged, and washed by MeOH solution.

3.3 Universal Approach to the Synthesis of the DFNS-Modified α -Cyclodextrin

1.22 g α -cyclodextrin (1.0 mmol) as well as 0.21 g *N,N'*-dicyclohexylcarbodiimide (1.0 mmol) were dissolved in 30 mL DMF in the presence of a small amount of 4 Å molecular sieves Ar. 0.25 g DFNS/Aniline was dissolved in 10 mL DMF, and then released dropwise in the solution. The reaction whisked was stirred two times, each for 48 h in an ice bath at 25 °C. Then, it set aside for 5 h until the precipitate was completely settled. The precipitate was separated using filtration. Next, the remaining sediment was poured

into 150 mL of acetone. The precipitate formed in acetone was collected using filtration.

3.4 Universal Approach to the Synthesis of the DFNS/ α -CD/Au NPs

200 mg DFNS/ α -CD and 0.027 mmol HAuCl₄·3H₂O (10 mM, 2.67 mL) were released in the suspension. The mixture was stirred continually for 1 h at 25 °C. The fresh solution of ice-cold NaBH₄ (30 mM, 2.65 mL, 0.08 mmol) was added dropwise to the suspension. The colour of the solution changed rapidly to red. The resulting solid was separated by centrifugation, washed by DI (deionized water) as well as ethanol, and then dried overnight at 40 °C.

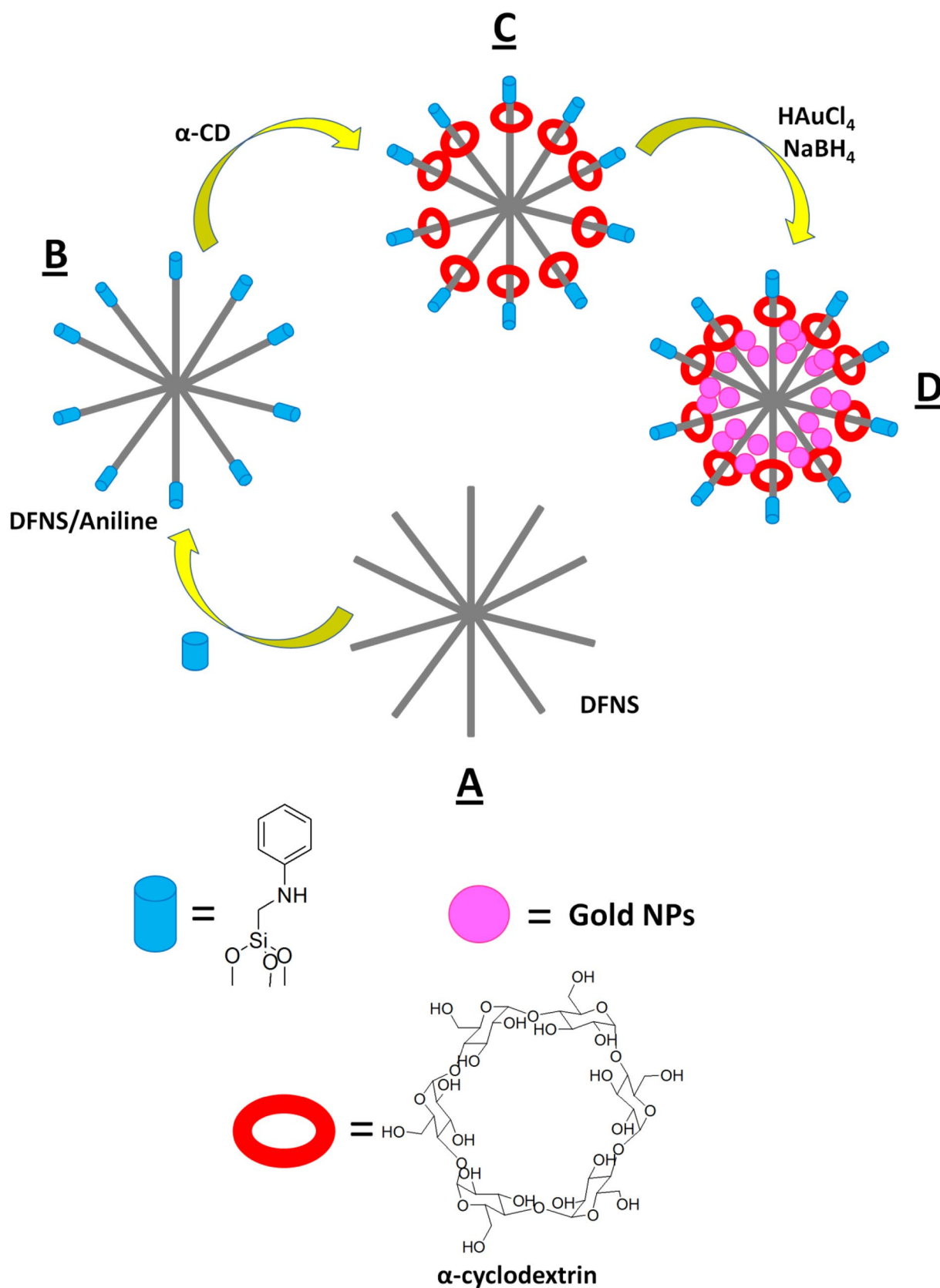
3.5 Universal Approach to the Synthesis of the 3a,4-Dihydronaphtho[2,3-c]furan-1(3H)-Ones

20 mg of DFNS/ α -CD/Au NPs, 1.0 mmol of cinnamyl chloride, and 1.0 mmol of phenylacetylene were poured in the reactor vessel without the use of any co-solvent. The reactor vessel was then subjected to continuous pressure with carbon dioxide and K₂CO₃ (1.0 mmol), and then heated at 90 °C for 30 min. Upon completion, reaction progress was analysed using TLC. EtOH was released in the DFNS/ α -CD/Au NPs and the reaction mixture was vacuum-filtered. The resulting solvent was removed and the product was purified by recrystallization using n-hexane/ethyl acetate.

4 Results and Discussion

In this paper, we hypothesized that gold NPs can be loaded into DFNS fibres (Step D), and that placing gold nanoparticles among DFNS fibres through DFNS blocking can prevent the release of gold through the fibres. This occlusion was performed using α -cyclodextrin (α -CD) (Step C) via an aniline bond as an interface (Step B) (Scheme 2).

The structures and morphologies of the DFNS, DFNS/ α -CD, and DFNS/ α -CD/Au NPs were characterized using SEM and TEM. Figure 1a depicts a picture of TEM (DFNS samples) by corrugated radial structures of uniform spheres (350 nm in diameter) and high-quality textures. Wrinkled fibres with a thicknesses of about 9 nm were observed. The fibres are arranged in 3D from the centre after growth. Moreover, the open pores were made conically using radial structures. The SEM image demonstrates the solid fibre nature of the whole sphere (Fig. 1d). In addition, increasing access to active surfaces as well as mass transfer of the reactants through the open channel of the mentioned hierarchical fibre structure was facilitated. The TEM and SEM images of DFNS/ α -CD NPs proved that, after modification,



Scheme 2 Schematic description of the synthesis of DFNS/ α -CD/Au NPs

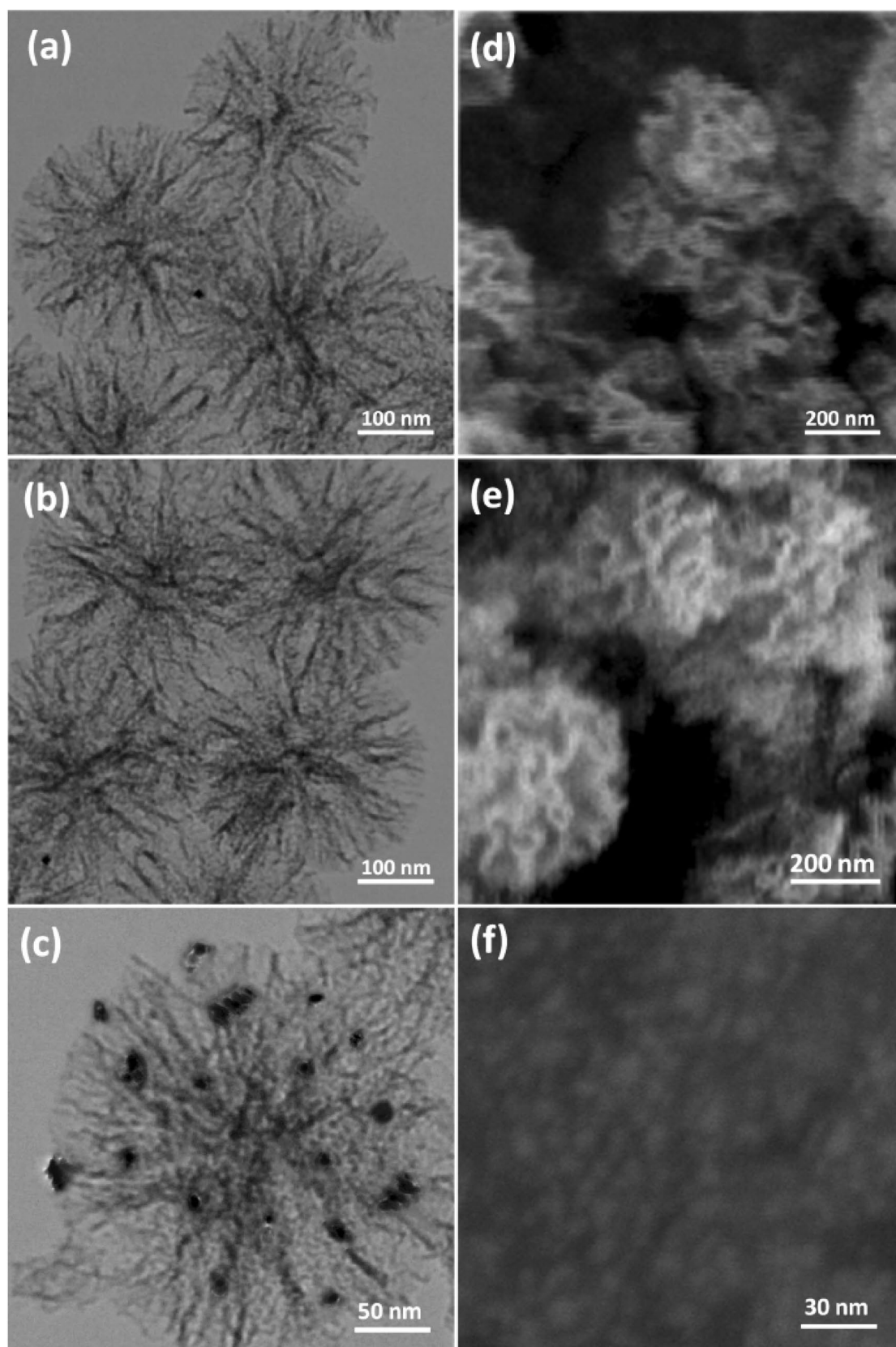


Fig. 1 TEM photos of DFNS NPs (a); DFNS/ α -CD NPs (b); DFNS/ α -CD/Au NPs (c); FESEM images of DFNS NPs (d); DFNS/ α -CD NPs (e); and DFNS/ α -CD/Au NPs (f)

the morphology of DFNS did not differ (Fig. 1b, e). Figure 1c, f illustrate that FESEM and TEM photos of the Au NPs. As observed, the as-prepared metal NPs were spherical without considerable aggregation. The Au diameter NPs was 10–20 nm. Here, NPs were attached to the DFNS wall.

Figure 2 shows the XRD pattern of DFNS and DFNS/ α -CD/Au NPs. The broad peak in the range of 20–30° is related to amorphous silica as opposed to the XRD pattern of DFNS NPs (refer to Fig. 2a). In addition, Fig. 2b shows the peaks of $2\theta = 38.1^\circ$, 44.3° , 64.5° , and 77.7° , which reflect the presence of gold nanoparticles in the structure of DFNS/ α -CD/Au catalyst (JCPDS 04-0784). This proves the development of gold particles on the surface of DFNS/ α -CD. The wide peak in the range of 20–30° belongs to amorphous silica. XRD analysis may simply be indexed for the cubic phase of gold NPs. Figure 2b demonstrates the presence of Au nanoparticles [sharp peaks of (111), (200), (220), (311), and (222)].

Thermogravimetric analysis of this material was done at different temperatures (from room temperature to 700 °C) to confirm the thermal stability of DFNS/ α -CD/Au nanoparticles (refer to Fig. 3). Weight reduction at 180 °C was due to the removal of both physisorbed and chemisorbed solvents on the surface of the silica material. Organic weight reductions (in range of 200–410 °C) of DFNS/*N*-phenylaminomethyl/ α -CD and DFNS/*N*-phenylaminomethyl NPs are 28.3% and 9.7%, respectively. The results confirm the organic structures supported on the DFNS surface.

The representative spectra of FT-IR of DFNS as well as DFNS/ α -CD/Au are represented in Fig. 4. The bands perceived at 1628, 805, and 1106 cm^{-1} in the FT-IR spectrum for DFNS and DFNS/ α -CD/Au showed that is belonged to the tensile state of the normal silanol group (Si–OH), the water absorbed on the solid surface, and Si–O–Si vibrations,

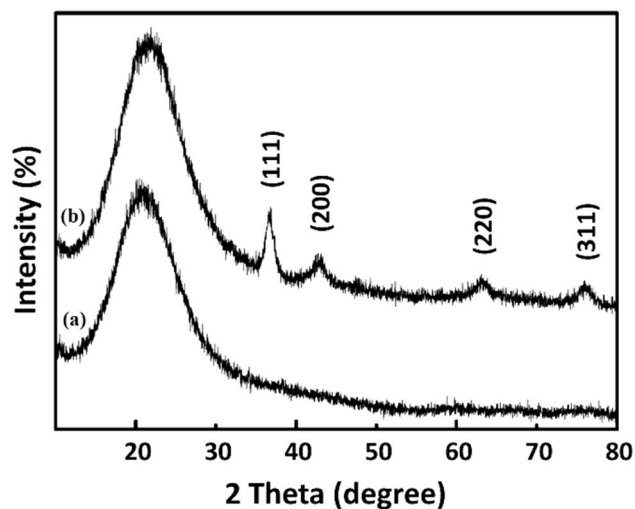


Fig. 2 XRD analysis of (a) DFNS, and (b) DFNS/ α -CD/Au

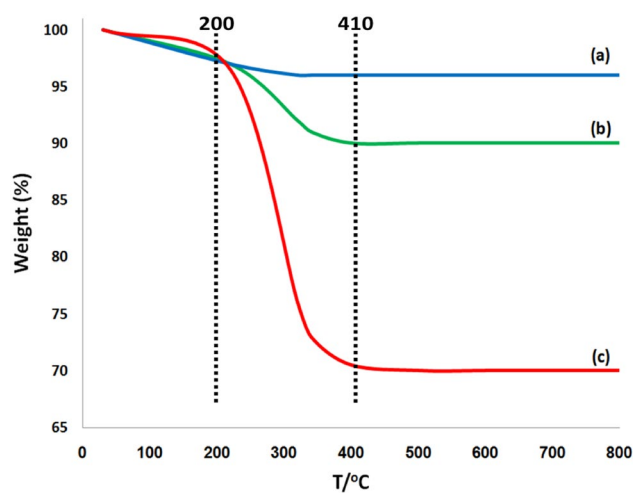


Fig. 3 TGA diagram of (a) DFNS, (b) DFNS/*N*-phenylaminomethyl, and (c) DFNS/*N*-phenylaminomethyl/ α -CD NPs

respectively. The DFNS/ α -CD/Au composite indicates bands at about 1094, 795 and 464 cm^{-1} . The broad and strong absorption band (at 3000–3540 cm^{-1}) is belonged to the -OH tensile vibrations. In addition, the narrow peak of about 2940 cm^{-1} is related to -CH fragments. The characteristic absorption bands belong to the O–C–O moiety in α -CD (1080–1125 cm^{-1}), which stands in the DFNS/ α -CD/Au range of material. It should be noted that, the absorption band of about 1700–1730 cm^{-1} was attributed to the carbamate-type association between cellulose and α -CD.

The total pore volume, BJH pore diameter, and BET surface area were 1.51 cm^3/g , 13.64 nm, and 497 m^2/g . The factors related to DFNS/ α -CD NPs reduced to 1.03 cm^3/g , 10.21 nm, and 402 m^2/g for DFNS. DFNS/ α -CD nitrogen uptake evaluation. Furthermore, a uniform structure with reduced pore diameter, surface area, and pore volume factors was recorded compared to pristine DFNS. The pore volume

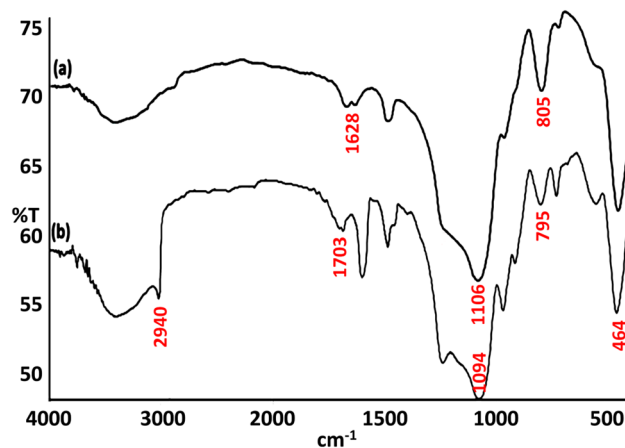
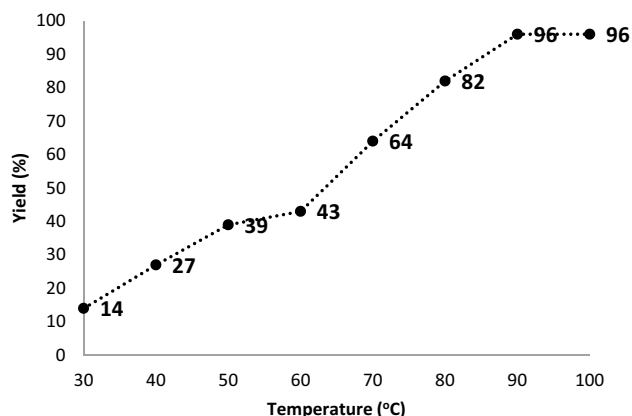


Fig. 4 FTIR spectra of (a) DFNS, and (b) DFNS/ α -CD/Au

Table 1 Structural parameters of DFNS, DFNS/ α -CD, and DFNS/ α -CD/Au materials determined from nitrogen uptake experiments

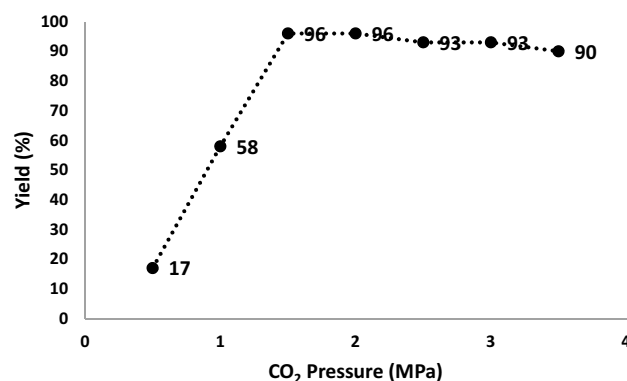
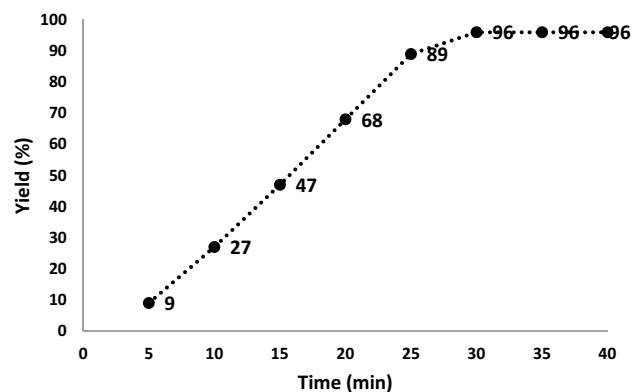
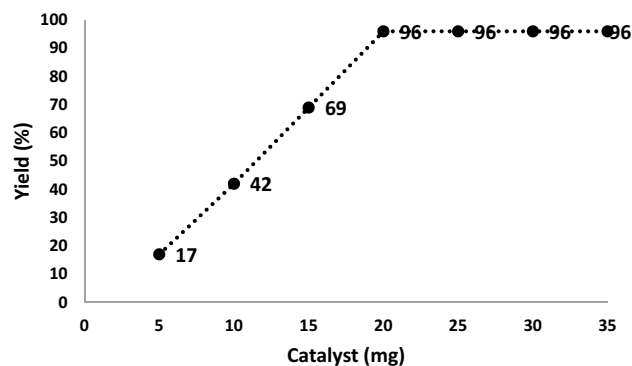
Catalysts	S_{BET} (m ² g ⁻¹)	V_t (cm ³ g ⁻¹)	D_{BJH} (nm)
DFNS	497	1.51	13.64
DFNS/ α -CD	402	1.03	10.21
DFNS/ α -CD/Au	296	0.68	5.13

**Fig. 5** Influence of reaction temperature

decreased significantly with increasing *N*-phenylaminomethyl as well as α -CD into the catalyst structure. It can be attributed to the high load of sensing probe that occupies a large volume in the silicate walls. The formation of Au NPs further reduced the porosity properties. It is interesting to note that a decrease in pore volume was observed at the time of gold nanoparticles formation (from 1.03 cm³g⁻¹ of DFNS/ α -CD to 0.68 cm³g⁻¹ of DFNS/ α -CD/Au). This reduction proved the placement of gold nanoparticles among DFNS fibres (refer to Table 1).

Temperature has been shown to dramatically accelerate the reaction. Through the lens of practical utilization, heat elimination is crucial to conserve energy since the reaction of CO₂ insertion in alkynes is significantly exothermic. Reaction yields increased from 14% to 96% in at 30–90 °C during 0.5 h. When the temperature was raised to 90–100 °C, no significant increase in the reaction of cinnamyl chloride, and phenylacetylene with CO₂ yield was observed. Through the lens of energy saving, 90 °C was identified as the best temperature for reaction (Fig. 5).

Figure 6 shows the influence of CO₂ pressure. Increasing the concentration of CO₂ in the reaction phase increased the yield of 3a,4-dihydronaphtho[2,3-*c*]furan-1(3*H*)-ones. Therefore, by increasing the CO₂ pressure from 0.5 MPa to 1.5 MPa, the yield of product gradually increased. The 3a,4-dihydronaphtho[2,3-*c*]furan-1(3*H*)-one concentration was decreased and reduced the reaction activity by further enhancing the CO₂ pressure to 2.5 MPa. In Fig. 7

**Fig. 6** The influence of CO₂ pressure**Fig. 7** The influence of reaction time**Fig. 8** The influence of catalyst amount

shows the yield dependency of 3a,4-dihydronaphtho[2,3-*c*]furan-1(3*H*)-one on the reaction time. The yield of 3a,4-dihydronaphtho[2,3-*c*]furan-1(3*H*)-ones was considerably enhanced in 5–30 min, and there was no considerable alteration with prolongation of the of reaction time. The reaction was completed in approximately 30 min. As shown in Fig. 8, the yield of 3a,4-dihydronaphtho[2,3-*c*]furan-1(3*H*)-ones

was enhanced with increasing DFNS/ α -CD/Au NPs catalyst value. No product was obtained in the absence of the catalyst. The result of adding 10–15 mg of catalyst to the sample reaction was the average yield of product. The best result was achieved in the presence of 20 mg of catalyst.

The catalytic activities were studied under optimal reaction conditions to investigate the amplitude and limitations of the DFNS/ α -CD/Au NPs (refer to Table 2). Alkynes bearing an electron-donating substituent (Table 2, entries 2 and 3) were changed to 3a,4-dihydronaphtho[2,3-c]furan-1(3*H*)-ones in high efficiencies. In order to obtain the product in a good yield that is likely because of the reduced electron density of the alkynes nitrogen atom, an electron-withdrawing group considered for alkynes (Table 2, entries 4 and 5).

To further examine the performance of the catalyst, various control tests were done and the related information is illustrated in Table 3. First, a standard reaction was performed utilizing DFNS. Results showed that no value of the favorable product was produced after 30 min of reaction time (Table 3, entry 1). In addition, when DFNS/ α -CD was deployed as a catalyst, a no reaction was observed (Table 3, entry 2). The DFNS or α -CD could not provide sufficient catalytic activity under mild reactions. Concerning these unsatisfactory results, we continued research to enhance the efficiency by adding Au NPs (Table 3, entry 3). Our results show that the reaction cycle was primarily catalysed deploying the types of Au NPs supported in the DFNS nanostructure. Nano-sized particles enhance the amount of catalyst activity due to the increase in surface area to volume, so they significantly increase the sensitivity between the reactants and the catalyst and act like a homogeneous catalysts.

In green chemistry, for reaction of allylic chlorides and alkynes by CO_2 , the reusability of a catalyst is introduced as an important feature. Hence, reusability of the DFNS/ α -CD/Au NPs was investigated considering optimized mode. The DFNS/ α -CD/Au NPs were directly separated from the liquid reaction after a completed run of reaction. After cleaning the catalysts, the compound can be reused immediately. Figure 9 shows that the catalyst was reused for ten continuous runs. We have obtained 91% of product at the 10th run, which shows only a 5% drop in performance compared to 96% of fresh catalyst. Besides, for the production of 3a,4-dihydronaphtho[2,3-c]furan-1(3*H*)-one the value of Au leached in the solution was evaluated using ICP after each run. Figure 10 shows that reuse of the catalyst in ten consecutive runs did not reduce catalytic activity, considering minimal (<0.05 ppm) leaching of Au (as investigated by ICP-OES).

Furthermore, a comprehensive study was conducted to demonstrate the catalyst heterogeneous nature. First, the hot filtration test for the synthesis of 3a,4-dihydronaphtho[2,3-c]furan-1(3*H*)-one demonstrated that the catalyst is removed after 15 min at a yield of 47%. The outcomes proved that,

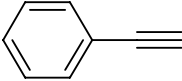
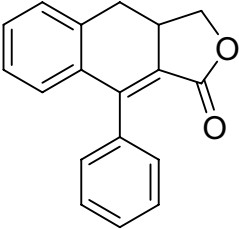
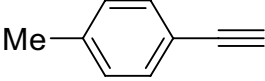
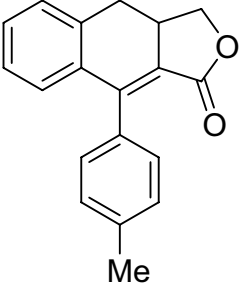
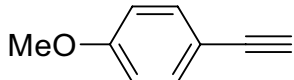
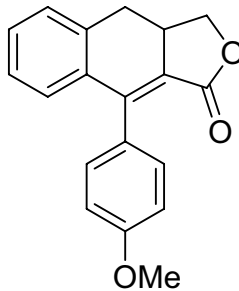
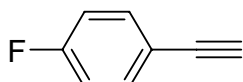
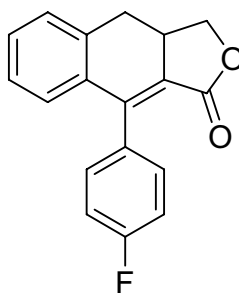

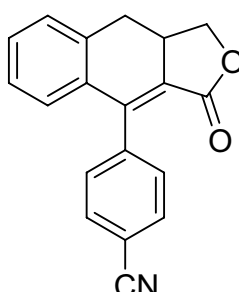
after utilizing the heterogeneous catalyst, the amount of gold nanoparticles leaching from the surface of the DFNS and remaining in the reaction mixture was very low. After 30 min, the product was acquired with 49% efficiency. In the process of reaction, it was proved that the catalyst acts heterogeneously and only a slight leaching was observed in the reaction. Second, to prove the heterogeneous pattern of the catalyst, we carried out the mercury poisoning investigation. Mercury (0) is dramatically deactivated the metal catalyst (active surface) and blunted the catalyst activity. The experimental set in this research proved the catalyst heterogeneous behavior. After 15 min of the reaction, about 300 M mercury was released to the reaction compound. For more than 30 min, the reaction area was stirred. After 30 min of catalyst poisoning, no more conversion was perceived. Figure 11 indicates the kinetics form of the reaction in the presence of Hg (0). Negative results of heterogeneity tests (Hg (0) poisoning as well as hot filtration), illustrated that the solid catalyst is completely heterogeneous and no acquirable gold leaching happened upon the synthesis of 3a,4-dihydronaphtho[2,3-c]furan-1(3*H*)-one.

The Au NPs load in the DFNS/ α -CD/Au and DFNS/Au NPs was determined by ICP-MS as 1.9 and 2.0%, respectively. Almost equal load values were obtained in both nanocomposites. In addition, leaching of gold NPs was investigated by the ICP-MS analysis of the catalyst after ten reaction cycles. The amount of Au NPs in the DFNS/ α -CD/Au NPs after ten reuse was 1.7%, which showed a negligible Au NPs leaching. The amount of Au NPs in the DFNS/Au NPs was 0.8%, indicating leaching of Au NPs. This remarkable ability of the DFNS/ α -CD/Au structure can be attributed to the α -CDs, which were able to effectively reacted by preventing the accumulation of Au NPs and the releasing and retrieval of Au NPs during the reaction process (Table 4). Comparison of TEM images of the utilized catalyst (Fig. 12a) with the fresh catalyst (Fig. 1f) shows a decrease in the number of gold nanoparticles among the fibers of DFNS/Au NPs after ten times recycling. However, application of DFNS/ α -CD/Au NPs did not change the number of gold nanoparticles (Fig. 12b). The structural stability of DFNS/ α -CD/Au NPs was due to the presence of α -CD in the catalyst anatomy.

5 Conclusions

In this paper, a series of DFNS/ α -CD/Au NPs catalysts were provided using in situ gold NPs on the DFNS surface. DFNS/ α -CD/Au catalysts with proper mesoporous structure along with the α -CD species were properly incorporated into the DFNS framework. To form smaller Au particles and enhance the surface area of the catalysts, increasing the amount of α -CD doping rate was

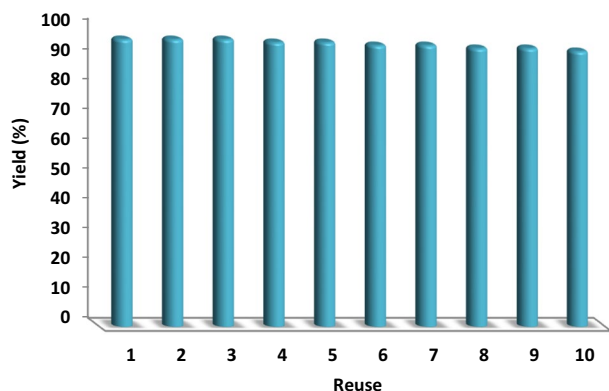
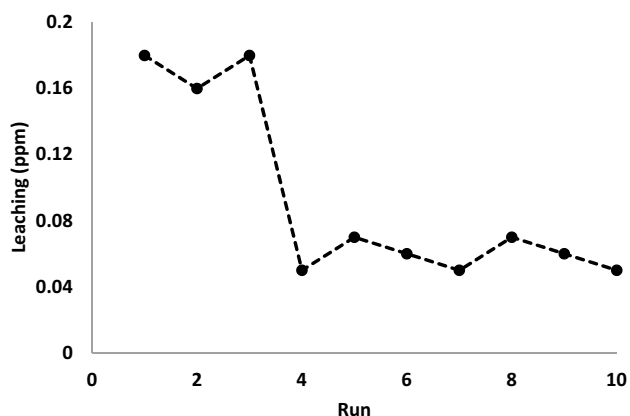
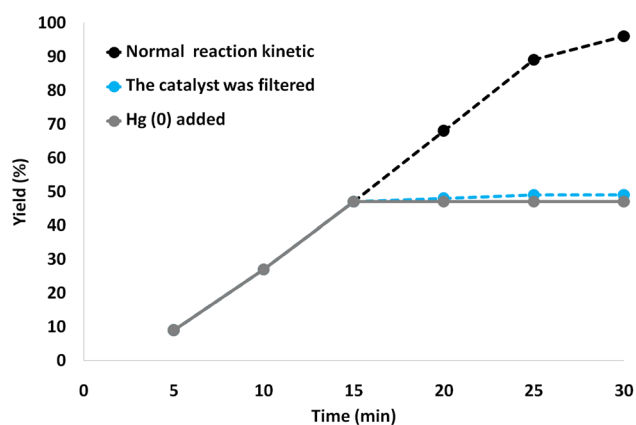
Table 2 Synthesis of 3a,4-dihydronaphtho[2,3-c]furan-1(3*H*)-one derivatives in the presence of DFNS/ α -CD/Au NPs^a

Entry	Alkynes	Products	Yield (%) ^b
1			96
2			97
3			98
4			92
5			91

^aReaction states: The blend of allylic chlorides (1.0 mmol), alkynes (1.0 mmol), and DFNS/ α -CD/Au NPs (20 mg), K₂CO₃ (1.0 mmol), CO₂ (1.5 MPa) for 30 min at 90 °C^bIsolated yields

Table 3 Influence of different catalysts for synthesis of 3a,4-dihydronaphtho[2,3-c]furan-1(3*H*)-one

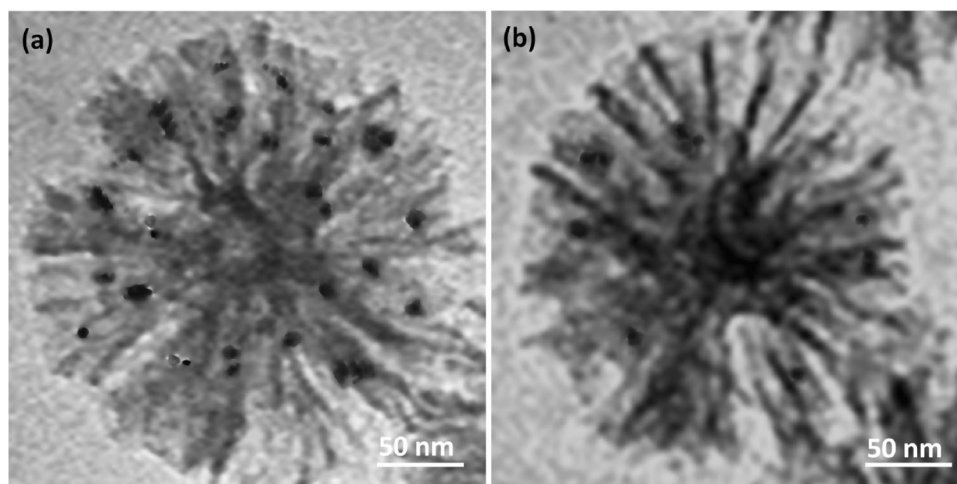
Entry	Catalyst	Yield (%) ^a
1	DFNS	—
2	DFNS/ α -CD	—
3	DFNS/ α -CD/Au	96

^aIsolated yield**Fig. 9** Reusability of catalysts for the synthesis of 3a,4-dihydronaphtho[2,3-c]furan-1(3*H*)-one. The DFNS/ α -CD/Au NPs were separated after a completed run of reaction, then cleaned and used for recyclability tests**Fig. 10** Recyclability of the catalyst for synthesis of 3a,4-dihydronaphtho[2,3-c]furan-1(3*H*)-one**Fig. 11** Reaction kinetics, Hg(0) poisoning, and hot filtration studies for synthesis of 3a,4-dihydronaphtho[2,3-c]furan-1(3*H*)-one**Table 4** The loading amount of Au NPs

Entry	Catalyst	wt%
1	DFNS/ α -CD/Au	1.9
2	DFNS/Au	2.0
3	DFNS/ α -CD/Au after ten reuses	1.7
4	DFNS/Au after ten reuses	0.8

appropriate. The gold NPs acted as the active sites. Furthermore, the synthesized DFNS/ α -CD/Au NPs were found to have excellent catalytic properties in the reduction synthesis of 3a,4-dihydronaphtho[2,3-c]furan-1(3*H*)-one. Therefore, any other promising NPs with proper properties, such as reusability and high efficiency, can be expanded in the future by pursuing the method proposed in this study.

Fig. 12 TEM images of the recovered DFNS/ α -CD/Au NPs (a), and DFNS/Au (b) after the 10th run for oxidation of phenol



Acknowledgements The authors are grateful for the financial support provided by the National Natural Science Foundation of China (No. 51908211).

References

- Devens G, Moore TA, Moore AL (2009) *Acc Chem Res* 42:1890–1898
- Morris AJ, Meyer GJ, Fujita E (2009) *Acc Chem Res* 42:1983–1994
- Morimoto T, Nishiura C, Tanaka M, Rohacova J, Nakagawa Y, Funada Y, Koike K, Yamamoto Y, Shishido S, Kojima T, Saeki T, Ozeki T, Ishitani O (2013) *J Am Chem Soc* 135:13266–13269
- Tanaka K, Ooyama D (2002) *Coord Chem Rev* 226:211–218
- Benson EE, Kubiak CP, Sathrum AJ, Smieja JM (2009) *Chem Soc Rev* 38:89–99
- Sato S, Morikawa T, Saeki S, Kajino T, Motohiro T (2010) *Angew Chem Int Ed* 49:5101–5105
- Thoi VS, Chang CJ (2011) *Chem Commun* 47:6578–6580
- Kudo A, Miseki Y (2009) *Chem Soc Rev* 38:253–278
- Qu Y, Duan X (2013) *Chem Soc Rev* 42:2568–2580
- Zhang J, Chen G, Chaker M, Rosei F, Ma D (2013) *Appl Catal B Environ* 132:107–115
- Saadati SM, Sadeghzadeh SM (2018) *Catal Lett* 148:1692–1702
- Gulati U, Rajesh UC, Rawat DS, Zaleski JM (2020) *Green Chem* 22:3170–3177
- Greve S, Friedrichsen W (1999) *Prog Heterocycl Chem* 11:144–162
- Greve S, Friedrichsen W (2000) *Prog Heterocycl Chem* 12:134–160
- Ito C, Katsuno S, Kondo Y, Tan HTW, Furukawa H (2000) *Chem Pharm Bull* 48:339–343
- Correa J, Romo J (1966) *Tetrahedron* 22:685–692
- Hirai KI, Kayama J, Pan JH (1999) *Cancer Detect Prev* 23:539–550
- Wang ML, Jiang TT, Lu Y, Liu HJ, Chen Y (2013) *J Mater Chem A* 1:5923–5933
- Zhang X, Su Z (2012) *Adv Mater* 24:4574–4577
- Sadeghzadeh SM, Daneshfar F, Malekzadeh M (2014) *Chin J Chem* 32:349–355
- Liu YM, Tsunoyama H, Akita T, Xie SH, Tsukuda T (2011) *ACS Catal* 1:2–6
- Yang X, Huang C, Fu ZY, Song HY, Liao SJ, Su YL, Du L, Li XJ (2013) *Appl Catal B Environ* 140:419–425
- Zhong ZY, Lin JY, Teh SP, Teo J, Dautzenberg FM (2007) *Adv Funct Mater* 17:1402–1408
- Wang F, Liu X, Lu CH, Willner I (2013) *ACS Nano* 7:7278–7286
- Miyamura H, Matsubara R, Miyazaki Y, Kobayashi S (2007) *Angew Chem Int Ed* 46:4151–4154
- Gu H, Wang J, Ji Y, Wang Z, Chen W, Xue G (2013) *J Mater Chem A* 1:12471–12477
- Wang X, Liu H, Chen D, Meng X, Liu T, Fu C, Hao N, Zhang Y, Wu X, Ren J, Tang F (2013) *ACS Appl Mater Inter* 5:4966–4971
- Chang YC, Chen DH (2009) *J Hazard Mater* 165:664–669
- Wang SN, Zhang MC, Zhang WQ (2011) *ACS Catal* 1:207–211
- Gangula A, Podila R, Ramakrishna M, Karanam L, Janardhana C, Rao AM (2011) *Langmuir* 27:15268–15274
- Gomez-Quero S, Cardenas-Lizana F, Keane MA (2013) *J Catal* 303:41–49
- Xu X, Fu Q, Guo X, Bao X (2013) *ACS Catal* 3:1810–1818
- Nie XT, Qian HF, Ge QJ, Xu HY, Jin RC (2012) *ACS Nano* 6:6014–6022
- Anand N, Ramudu P, Reddy KHP, Rao KSR, Jagadeesh B, Babu VSP, Burri DR (2013) *Appl Catal A Gen* 454:119–126
- Sadeghzadeh SM, Zhiani R, Emrani S (2018) *Catal Lett* 148:119–124
- Wang L, Wang H, Hapala P, Zhu LF, Ren LM, Meng XJ, Lewis JP, Xiao FS (2011) *J Catal* 281:30–39
- Delidovich IV, Moroz BL, Taran OP, Gromov NV, Pyrjaev PA, Prosvirin IP, Bukhtiyarov VI, Parmon VN (2013) *Chem Eng J* 223:921–931
- Sadeghzadeh SM (2015) *RSC Adv* 5:68947–68952
- Lin Y, Qiao Y, Wang Y, Yan Y, Huang J (2012) *J Mater Chem* 22:18314–18320
- Storaro L, Lenarda M, Moretti E, Talon A, Porta F, Moltrasio B, Canton P (2010) *J Coll Interf Sci* 350:435–442
- Xu LX, He CH, Zhu MQ, Fang S (2007) *Catal Lett* 114:202–205
- Liu RH, Gao NS, Zhen F, Zhang YY, Mei L, Zeng XW (2013) *Chem Eng J* 225:245–253
- Sobczak I, Kusior A, Grams J, Ziolk M (2007) *J Catal* 245:259–266
- Selvakannan PR, Mantri K, Tardio J, Bhargava SK (2013) *J Coll Interf Sci* 394:475–484
- Polshettiwar V, Cha D, Zhang XX, Basset JM (2010) *Angew Chem Int Ed* 49:9652–9656

46. Lilly Thankamony AS, Lion C, Pourpoint F, Singh B, Perez Linde AJ, Carnevale D, Bodenhausen G, Vezin H, Lafon O, Polshettiwar V (2015) *Angew Chem Int Ed* 54:2190–2193
47. Bouhrara M, Ranga C, Fihri A, Shaikh RR, Sarawade P, Emwas AH, Hedhili MN, Polshettiwar V (2013) *ACS Sustain Chem Eng* 1:1192–1199
48. Dhiman M, Chalke B, Polshettiwar V (2015) *ACS Sustain Chem Eng* 3:3224–3230
49. Fihri A, Bouhrara M, Cha D, Almana N, Polshettiwar V (2012) *ChemSusChem* 5:85–89
50. Mahato SK, Bhaumik M, Maji A, Dutta A, Maiti D, Maity A (2018) *J Colloid Interface Sci* 513:592–601
51. Jayarajan R, Kumar R, Gupta J, Dev G, Kadu P, Chatterjee D, Bahadur D, Maiti D, Maji SK (2019) *J Mater Chem A* 7:4486–4493
52. Kundu PK, Dhiman M, Modak A, Chowdhury A, Polshettiwar V, Maiti D (2016) *ChemPlusChem* 81:1142–1146
53. Das J, Dolui P, Ali W, Biswas JP, Chandrashekar HB, Prakasha G, Maiti D (2020) *Chem Sci* 11:9697–9702
54. Chen Y, Liu Y, Mao D, Yu J, Zheng Y, Guo X, Ma Z (2020) *J Taiwan Inst Chem Eng* 113:16–26
55. Bai L, Wyrwalski F, Franc J, Lamonier O, Khodakov AY, Monflier E, Ponchel A (2013) *Appl Catal B Environ* 138–139:381–390
56. Bai L, Wyrwalski F, Safariamin M, Bleta R, Lamonier JF, Przybylski C, Monflier E, Ponchel A (2016) *J Catal* 341:191–204
57. Karnjanakom S, Guan GQ, Asep B, Hao XG, Kongparakul S, Samart C, Abudula A (2016) *J Phys Chem C* 120:3396–3407
58. Wu H, Liu J, Liu H, He D (2019) *Fuel* 235:868–877
59. Fihri A, Bouhrara M, Patil U, Cha D, Saih Y, Polshettiwar V (2012) *ACS Catal* 2:1425–1431
60. Dibenedetto A, Angelini A, Stufano P (2014) *J Chem Technol Biot* 89:334–353
61. Low JX, Cheng B, Yu JG (2017) *Appl Surf Sci* 392:658–686
62. Boot-Handford ME, Abanades JC, Anthony EJ, Blunt MJ, Brandani S, Mac Dowell N, Fernandez JR, Ferrari MC, Gross R, Hallett JP, Haszeldine RS, Heptonstall P, Lyngfelt A, Makuch Z, Mangano E, Porter RTJ, Pourkashanian M, Rochelle GT, Shah N, Yao JG, Fennell PS (2014) *Energy Environ Sci* 7:130–189

Publisher's Note Springer Nature remains neutral with regard to jurisdictional claims in published maps and institutional affiliations.